

Modified neural network based cascaded control for product composition of reactive distillation

Vandana Sakhre^{1*}, Sanjeev Jain¹, V. S. Sapkal², D.P. Agarwal³

¹Madhav Institute of Technology & Science, Gwalior-474005, India

²SGB Amravati University, Amravati-444062, India

³IIT, New Delhi-110001, India

*Corresponding author: e-mail: vssakhre@gmail.com

In this research work, neural network based single loop and cascaded control strategies, based on Feed Forward Neural Network trained with Back Propagation (FBPNN) algorithm is carried out to control the product composition of reactive distillation. The FBPNN is modified using the steepest descent method. This modification is suggested for optimization of error function. The weights connecting the input and hidden layer, hidden and output layer is optimized using steepest descent method which causes minimization of mean square error and hence improves the response of the system. FBPNN, as the inferential soft sensor is used for composition estimation of reactive distillation using temperature as a secondary process variable. The optimized temperature profile of the reactive distillation is selected as input to the neural network. Reboiler heat duty is selected as a manipulating variable in case of single loop control strategy while the bottom stage temperature T₉ is selected as a manipulating variable for cascaded control strategy. It has been observed that modified FBPNN gives minimum mean square error. It has also been observed from the results that cascaded control structure gives improved dynamic response as compared to the single loop control strategy.

Keywords: composition, inferential control, neural network, reactive distillation, soft sensor.

INTRODUCTION

The Combination of reaction and separation in a single unit as in case of reactive distillation process is advantageous over conventional process for those reversible reactions in which equilibrium limits conversion. The continuous removal of product from reaction mixture also helps in improving selectivity. The *insitu* generated heat of reaction can also be effectively used in evaporation of the liquid phase. However, this combination of reaction and separation in a single unit operation leads to the highly nonlinear behavior of reactive distillation process. The control of such nonlinear process is a challenging task. Product composition measurements by online analyzers are not cost effective and also they do not give accurate measurements. Therefore, product composition can be measured based on measurement of secondary process variables. In case of reactive distillation process, temperature measurement can be used as a secondary process variable for measuring product composition. An inferential state estimator such as Neural Network can be effectively used to infer the product composition of reactive distillation process.

The work on control of reactive distillation process is reported since 1996. Sorensen et al.¹ has proposed optimal online operation and control of the reactive batch distillation process. They have determined optimal values for reflux ratio and reboiler heat duty based on maximum profit and minimum operating time and implemented this optimal policy for feedback control of the batch reactive distillation system. Al Arfaj and Luyben² have discussed six alternative control structures along with rigorous dynamic simulation for ideal two reactant two product reactive distillation column. Apart from using temperature measurement, they have explored a variety of control structure possibilities for control of different type of reactive distillation column. Kano et al.³ proposed Partial Least Square (PLS) regression to inferential

control of distillate composition. They have selected tray temperature, reflux flow and reboiler heat duty as a secondary process variables along with simulated time series data for development of the dynamic inferential model. Tight control of nonlinear reactive distillation is a difficult task. To have tight control of nonlinear batch reactive distillation, Doyle et al.⁴, has been developed low order model (reduced model) based on travelling wave phenomena. This reduced model used in nonlinear model predictive control for esterification reaction in batch column. To overcome with various disturbances and to maintain set point tracking in reactive distillation column, Tian et al.⁵ has developed Pattern-based Predictive Control (PPC) scheme based on Fuzzy logic rules. This scheme has been developed for control of the purity of the ETBE reactive distillation process. Lee et al.⁶, have proposed dynamics and control of three different flow sheets for esterification of acetic acid and the degree of process nonlinearity is analyzed qualitatively based on the residue curve map and the boiling point ranking and it can be computed quantitatively based on the fraction or based on Allgower's nonlinearity measure. The systematic design and dual temperature control and overall control strategy for different esterification process have studied by Huang et al.⁷, Chien et al.⁸. Similar work was also carried out using simple one tray temperature control by the following researchers^{9–11}. Dynamic model development and model predictive control, including neural network control studies have been carried out by many researchers^{12–21}. Adaptive Neural Network (ADALINE) and Dynamic ADALINE (D-ADALINE) as a soft sensor was developed by Rani et al.²².

Artificial Neural Network (ANN) as a soft sensor estimator have great potential for control of reactive distillation processes due to their nonlinear identification capabilities. In this research work, authors have implemented Feed Forward Back Propagation Neural

Network (FBPNN) which is modified using the steepest descent method is used as soft sensor for single loop and cascaded control strategies for control of reactive distillation process. For the representative process, propyl propionate synthesis via reactive distillation is chosen.

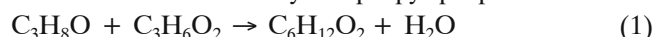
The aim of the present study is to control the product composition of reactive distillation using inferential soft sensor technique which is based on feed forward neural network trained using back propagation algorithm. The FBPNN is then modified using the steepest descent method which optimizes the error function and minimizes mean square error. The dynamic mathematical model which is an essential and powerful tool for simulation study is considered in the research work.

The organization of this paper is as follows: Process description and experimental synthesis is given in section 2. Section 3 comprises of nonlinear dynamic model equations. Description of FBPNN with its modified algorithm and control strategies using single loop and cascaded control is presented in section 4. The results and discussions are presented in section 5. The conclusion of the work is given in section 6.

PROCESS DESCRIPTION

Propyl propionate is a widely used solvent as polymerization solvent, automotive refinishing, and appliance coatings. It is considered as a non-hazardous air pollutant which makes it a good alternative for aromatic hydrocarbon solvents like toluene and xylene. Furthermore, it is used as an artificial flavor in the food industry. It is synthesized by the equilibrium-limited liquid-phase esterification reaction of 1-propanol and propionic acid. The standard enthalpy of reaction was experimentally determined to be -6.4 kJ/mol. This indicates that the reaction is exothermic and the chemical equilibrium constant is slightly dependent on temperature. The reaction is not self-catalyzed and needs to be catalyzed by a strong acidic catalyst²³.

The reaction chemistry for propyl propionate is:



Reaction Kinetics: For a heterogeneous catalyst such as Amberlyst 15, the rate is affected by the amount of catalyst used. The rate constants for both forward rate, k_f and reverse rate, k_r is obtained from data provided by Buchaly et al.²⁴. The rate can be written as follows:

$$R_{n,i} = (W \cdot v_{i,m})(k_f C_{PA} C_{POH} - k_r C_{PP} C_{H_2O}) / K_{eq} \quad (2)$$

$$k_f = 7.381 \cdot 10^7 \exp\left(-5.963 \cdot \frac{10^4}{RT}\right) \quad (3)$$

$$K_{eq} = 6.263 \exp\left(\frac{4.519 \cdot 10^3}{RT}\right) \quad (4)$$

Experimental Synthesis of Propyl Propionate

A pilot scale reactive distillation column is used to collect the actual practical data for temperature and composition. This temperature and composition data is used to train the neural network. The pictorial view of the pilot scale reactive distillation column is shown in Figure 1. The experimental condition and other details are tabulated in Table 1. The maximum composition obtained experimentally for propyl propionate is 0.842.



Figure 1. Pilot Scale Reactive Distillation Column

Table 1. Input condition and results of experiment setup

| Parameters | Values | |
|--------------------------------|------------------|----------------|
| | propanol | propionic acid |
| Input condition | 80°C | 50°C |
| Temperature | 0.05 L/min | 0.01 L/min |
| Flow rate | 9 | |
| Reflux ratio | Katapak-S | |
| Packing used | Amberlyst 15 Wet | |
| Catalyst used | 3 | 6 |
| Feed stage | 2 L | |
| Initial volume of the Reboiler | 2 kW | |
| Reboiler heat duty | -4.69 kW | |
| Condenser heat duty | 40.71 mole/hr | |
| Distillate rate | 366.35 mole/hr | |
| Reflux rate | 119.89°C | |
| Reboiler temperature | 7.6 mole/hr | |
| Bottom rate | 442.6 mole/hr | |
| Boil up rate | 58.24 | |
| Boil up ratio | | |

MODEL EQUATIONS

A nonlinear dynamic modeling for the synthesis of propyl propionate in reactive distillation has been formulated. The model equations developed is employed to simulate the dynamics of the reactive distillation column. These model equations have the main features of the reactive distillation column and represents essential dynamics of the system. The packed reactive distillation with input and output flow quantities are shown in Figure 2. As reactive distillation exhibits non-equilibrium condition, following are the assumptions made:

1. Assuming three zones existing in RDC: Reaction, rectifying and stripping section.
2. Constant relative volatility.
3. Variable Liquid and constant vapor holdup throughout the column.

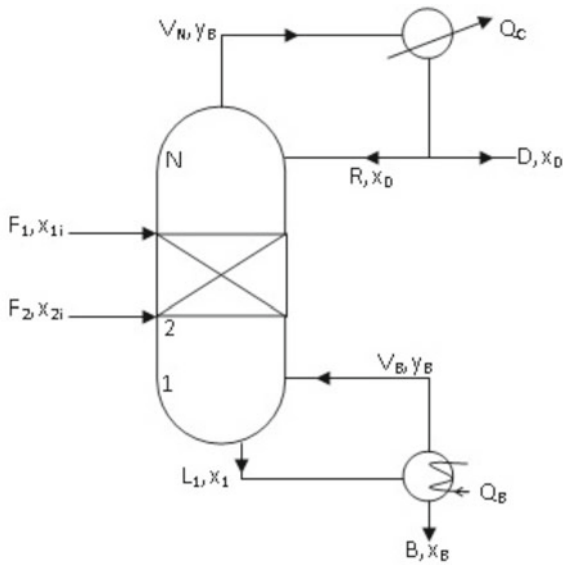


Figure 2. Packed Reactive Distillation Column with Flow Quantities

4. Complete mixing of vapor and liquid.

5. Chemical reaction occurs in liquid phase in reactive zone and in the reboiler. No reaction occurs in vapor phase.

Mass Balance: The component mass balance around the following sections is written as follows:

Reflux drum:

$$\frac{d(M_D x_{D,i})}{dt} = V_n y_{n,i} - D(1 + RR)x_{D,i} \quad (5)$$

Rectifying and stripping section:

$$\frac{d(M_n x_{n,i})}{dt} = (L_{n+1} x_{n+1,i} + V_{n-1} y_{n-1,i} - L_n x_{n,i} - V_n y_{n,i}) \quad (6)$$

Reactive section:

$$\frac{d(M_n x_{n,i})}{dt} = (L_{n+1} x_{n+1,i} + V_{n-1} y_{n-1,i} - L_n x_{n,i} - V_n y_{n,i} + R_{n,i}) \quad (7)$$

Feed section:

$$\frac{d(M_n x_{n,i})}{dt} = (L_{n+1} x_{n+1,i} + V_{n-1} y_{n-1,i} - L_n x_{n,i} - V_n y_{n,i} + \quad (8)$$

$$+ R_{n,i} + F_n z_{n,i}$$

Reboiler:

$$\frac{d(M_B x_{B,i})}{dt} = L_n x_{n,i} - B x_{B,i} - V_B y_{B,i} \quad (9)$$

Energy Balance: Assuming that change in enthalpy for rectifying and stripping section is constant, while it varies in the reactive zone because of exothermic heat of reaction involved in esterification reaction.

$$\frac{d}{dt}(V_R h_R) = V_{n+1} H_{n+1} + L_{n-1} h_{n-1} + F h_F - V_n H_n - \quad (10)$$

$$- L_n h_n - \lambda V_R R_{n,i}$$

Condenser Heat Duty:

$$Q_C = V_n H_n - (R_{rate} + D)h_D \quad (11)$$

Reboiler Heat Duty:

$$Q_B = B h_{B,i} + V_B h_{B,i} - L_n h_{n,i} \quad (12)$$

Rate of Heat and Mass Transfer

The vapor rate increases up through the reaction section and the liquid rate decreases down through the reactive section. Hence, in terms of heat of reaction involved with vapor and liquid flow rate, the equations can be written as:

$$V_n = V_{n-1} - \frac{\lambda}{\Delta H_v} R_{n,i} \quad (13)$$

$$(17)$$

$$L_n = L_{n+1} + \frac{\lambda}{\Delta H_v} R_{n,i} \quad (14)$$

The rate of mass transfer due to diffusion can be written as follows:

$$\frac{d}{dt}(V_M) = V_{n-1} y_{n-1} + L_{n+1} x_{n+1} - L_n x_n - V_n y_n + \quad (15)$$

$$+ \sum V_{i,m} E_K V_n$$

Temperature Measurement

The temperature measurement as a secondary variable and as an input for neural network estimator can be written for three stages selected as: the condenser and the reflux drum, the reactive stage and bottom reboiler temperature. For condenser, the change in temperature with time can be written as follows:

$$\frac{dT_n}{dt} = \frac{(L_{n-1} x_{n-1} - B x_B)(T_{n-1} - T_n)}{M_B} + \frac{Q_B}{M_B \cdot Cp} \quad (16)$$

The reaction stage temperature can be written as:

$$\frac{dT_n}{dt} = \frac{[(L_{n-1} x_{n-1})(T_{n-1} - T_n) + (V_{n+1} y_{n+1})(T_{n+1} - T_n) - (L_n x_n)(T_n - T_{n-1}) + (V_n y_n)(T_{n+1} - T_n) + (F x_{feed})(T_f - T_f)]}{M_f} + \frac{V_n \sum R_{n,i} T_R}{n}$$

For reboiler, the equation written is as follows:

$$\frac{dT_n}{dt} = \frac{(L_{n-1} x_{n-1} - B x_B)(T_{n-1} - T_n)}{M_B} + \frac{Q_B}{M_B \cdot Cp} \quad (18)$$

With the aid of MATLAB (R2013b), a program is developed for solving the above balance equations, rate equations and temperature equations using ode45 solver. Ode45 is an equation solver for solving stiff differential and algebraic equations.

FEED FORWARD BACK PROPAGATION NEURAL NETWORK (FBPNN)

The FBPNN is based on supervised learning. The feed forward back propagation neural network is a multilayer, feed forward consisting of an input layer, a hidden layer and an output layer and possesses weighted interconnections. The back propagation learning algorithm is applied to single layer feed forward network, which consist of processing elements with continuous differentiable activation function. For a given set of training input-output pair, this algorithm provides a procedure for changing weights in a BPN to classify the given input patterns correctly. The weight update algorithm is based on steepest descent method. This method is used where the error is propagated back to the hidden layer. The aim of this neural network is to train the net to achieve a balance between the net's ability to respond (memorization) and its ability to give a reasonable response to the input that is similar but not identical to the one that is used in training (generalization). The training of BPN is carried in three steps: the feed forward of the training input pattern, the calculation and back propagation of

the error and updation of weights. The testing of BPN involves the computation of feed-forward phase only²⁵. The modified diagram of FBPNN is shown in Figure 3.

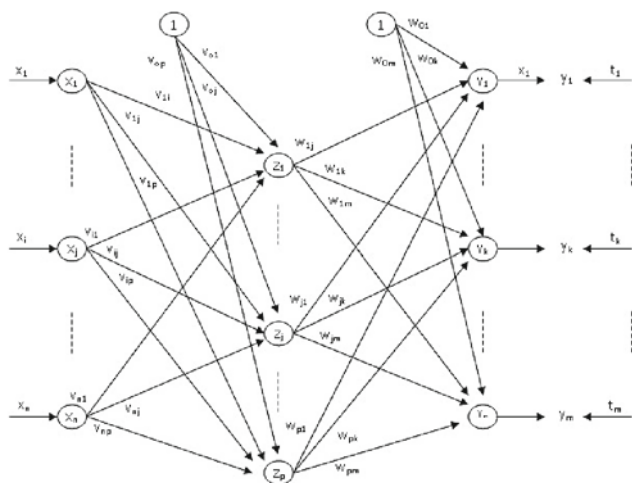


Figure 3. Modified Feed Forward Back Propagation Neural Network

FBPNN algorithm

FBPNN is used to control the product composition of propyl propionate reactive distillation process. The algorithm of FBPNN is modified with the steepest descent method. This modification is proposed for error function optimization to reduce mean square error. The steepest descent method is used to optimize the weights between input layer and hidden layer and between hidden and output layers. The proposed neural network algorithm is presented as below:

Let us consider given a input pattern:

$x = (x_1, x_2, \dots, x_n)$ and targets $t = (t_1, t_2, \dots, t_m)$.

x_i : represent i^{th} input unit,

t_j : represent j^{th} target unit,

v_{ij} : weight from i^{th} neuron at input layer and j^{th} neuron at hidden layer for $1 \leq i \leq N, 1 \leq j \leq P$.

v_{0j} : bias on j^{th} hidden unit,

w_{oj} : weight from j^{th} neuron at hidden layer and k^{th} neuron at output layer for $1 \leq j \leq P; 1 \leq k \leq N$.

Now calculate net input at j^{th} hidden neuron as follows:

$$z'_j = v_{0j} + \sum_{i=1}^n x_i v_{ij} \quad (19)$$

and

$$z_j = f(z'_j) \quad (20)$$

Where z_j denotes the output at j^{th} hidden neuron and f is activation function monotonically increasing and differentiable. Calculate the net input at k^{th} output neuron as follows:

$$y'_j = w_{ok} + \sum_{j=1}^p z_j w_{jk} \quad (21)$$

and

$$y_k = f(y'_k) \quad (22)$$

Where y_k denotes the output at k^{th} output neuron and f has its usual meaning.

The error at the k^{th} output node is:

$$e_k^p = t_k^p - y_k^p \quad (23)$$

where p denotes the given pattern.

Mean square error is given by:

$$E = \frac{1}{M} \sum_{k=1}^M \frac{1}{2} (e_k^p)^2 \quad (24)$$

During the training, the weights are updated after all the training pattern are fed into the inputs and thus the cost function becomes:

$$E = \frac{1}{PM} \sum_{p=1}^P \sum_{k=1}^M \frac{1}{2} (e_k^p)^2 \quad (25)$$

Optimization of Error Function Using Steepest Descent Method

Optimization of the error function is carried out to minimize mean square error. For this, we have optimized the weights at output and hidden layer, using the steepest descent method as follows:

1. For output layer: Differentiating equation (25) partially with respect to the weights w_{jk} we have:

$$\frac{\partial E}{\partial w_{jk}} = \frac{\partial E}{\partial e_j} \cdot \frac{\partial e_j}{\partial t_j} \cdot \frac{\partial t_j}{\partial \alpha_j} \cdot \frac{\partial \alpha_j}{\partial w_{jk}} = e_j \cdot (1) \cdot f'(\alpha_j) y_k \quad (26)$$

$$\frac{\partial E}{\partial w_{jk}} = e_j f'(\alpha_j) y_k$$

2. For hidden layer: Similarly, compute the partial derivative of Equation (25) with the weights v_{ij} we have:

$$\frac{\partial E}{\partial v_{ij}} = \sum_k \frac{\partial E}{\partial e_k} \cdot \frac{\partial e_k}{\partial \alpha_k} \cdot \frac{\partial \alpha_k}{\partial y_i} \cdot \frac{\partial y_i}{\partial \alpha_i} \cdot \frac{\partial \alpha_i}{\partial v_{ij}}$$

$$\text{or } \frac{\partial E}{\partial v_{ij}} = \sum_k e_k f'_k(\alpha_k) \cdot w_{jk} f'_i(\alpha_i) \cdot (-x_i) \quad (27)$$

$$\frac{\partial E}{\partial v_{ij}} = (-x_i) f'_i(\alpha_i) \sum_k e_k f'_k(\alpha_k) w_{jk}$$

Where f_i & f_k denotes an activation function. The optimization of the error function over the weights w_{jk} and v_{ij} is done by steepest-descent method in the direction of steepest descent:

$$\Delta w_{kj} = \eta \frac{\partial E}{\partial w_{jk}} \quad (28.a)$$

$$\Delta w_{kj} = \eta e_j f'(\alpha_j) y_k$$

and

$$\Delta v_{kj} = \eta \frac{\partial E}{\partial v_{ij}} \quad (28.b)$$

$$\Delta v_{ij} = -\eta x_i f'_i(\alpha_i) \sum_k e_k f'_k(\alpha_k) w_{jk}$$

Where η is known as learning rate.

Since steepest descent has a zigzag problem, to overcome this, we add a momentum term in Equation (28.a) and (28.b) at t^{th} iteration:

$$\Delta w_{jk}(t) = \eta \frac{\partial E(t)}{\partial w_{jk}} + \beta \Delta w_{jk}(t-1) \quad (29.a)$$

$$\Delta v_{ij}(t) = \eta \frac{\partial E(t)}{\partial v_{ij}} + \beta \Delta v_{ij}(t-1) \quad (29.b)$$

Where β is known as momentum constant and $\beta \in [0, 1]$. The graphical representation of steepest descent method is shown in Figure 4.

The modified algorithm of FBPNN is implemented in MATLAB. The optimal number of sensors used in this case is six temperatures from the reactive distillation process. These optimal temperatures are used as input to the neural network.

PID Controller

A proportional-integral-derivative (PID) controller is a feedback mechanism based control and widely used in industries. A PID controller calculates the error value as

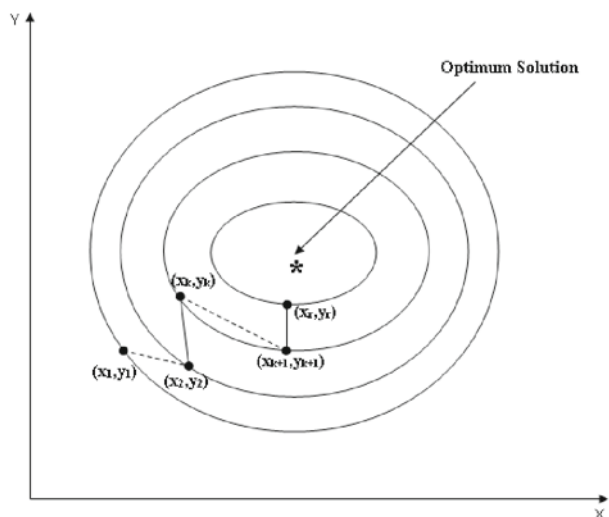


Figure 4. Graphical representation of steepest descent method (zigzag problem)

the difference between a measured process variable and a desired set point. The controller attempts to minimize the error by adjusting the process variable through the use of a manipulated variable.

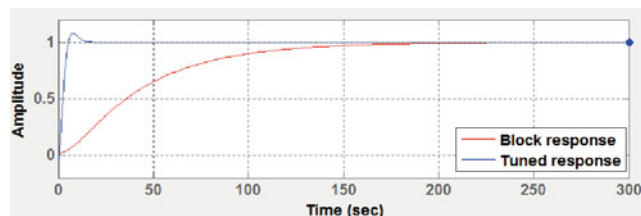
The output of the PID controller can be expressed as:

$$u(t) = k_p e(t) + k_i \int_0^t e(\tau) d\tau + k_d \frac{de}{dt} \quad (30)$$

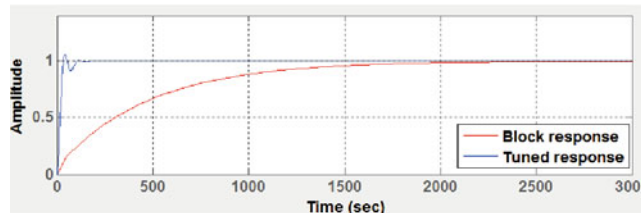
Where, u is the control signal, e is the error, τ is integral time and k_p , k_i and k_d proportional, integral and derivative gain respectively (Astrom & Hagglund)²⁶. All the three control combinations of conventional PID controller are used to control the reactive distillation process. The transfer function of the PID controller obtained is as follows:

$$G(s) = \frac{0.454(s+72.5)}{s(s+2.2)} \quad (31)$$

This controller is tuned using Tyreus-Luyben tuning method and the tuning parameters are $k_p = 205$ (gain), $\tau_i = 10$ min and $\tau_d = 1.27$ min. The PID controller tuning plots obtained for both single loop and cascaded control strategy is shown in Figures 5 (a) and (b) respectively. Rise time for single loop and cascaded loop are 3.53 and 22.1 seconds respectively. Settling time for both loops after tuning are 12.9 and 96.3 seconds



(a) Single Loop Control



(b) Cascaded Loop Control

Figure 5. PID Controller Tuning Response Curve

respectively. Percentage overshoot for both cases are observed as 7.99% and 5.26% respectively. This PID controller is designed to compensate error. The error generated during the process is sensed and compared with the reference value of the PID controller. Then the PID controller regulates the manipulating variable which is reboiler heat duty in this case.

Single Loop Control Strategy

The block diagram of the single loop control strategy is shown in Figure 6. Here, RDC(s) is the model of the reactive distillation column, FA and FB are the feed flow rate of the input feed A and B respectively. Based on four inputs, i.e. two feed flow rates FA and FB, reflux ratio and reboiler heat duty, six temperatures are obtained as output from the reactive distillation system. The two feed streams, and reflux ratio are the disturbing quantities considered. Reboiler heat duty is selected as manipulated variable. Product composition is selected as controlled variable. From the reactive distillation system, temperature change selected from six stages are taken as input to the neural network. These six temperatures are top stage temperature T1, four temperature T3, T4, T5 and T6 from reaction section and bottom stage temperature T9. These temperatures are used as secondary process variables for composition

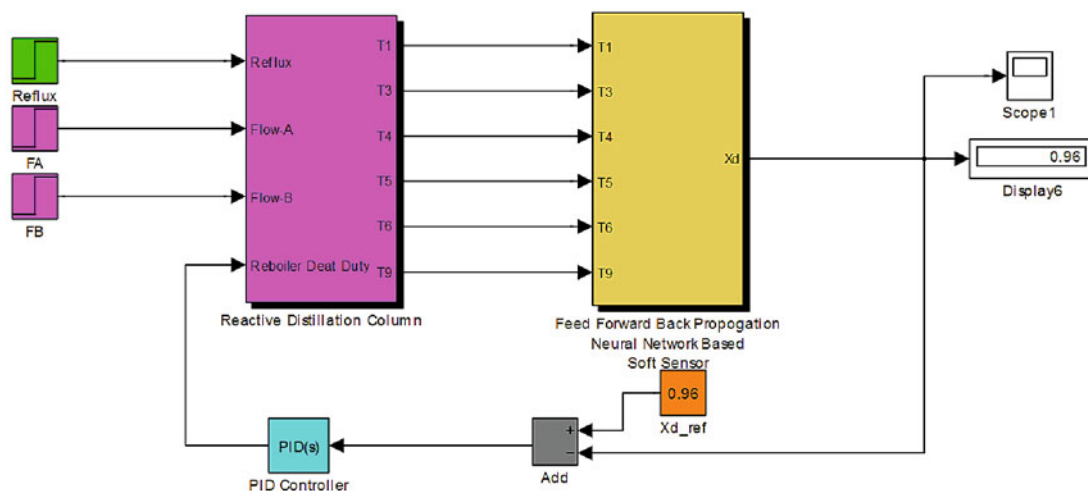


Figure 6. Single Loop Control of Reactive Distillation using modified FBPNN

measurement. Modified feed forward back propagation neural network with optimization of error function using the steepest descent method uses these temperature measurements from reactive distillation column as input to the neural network to estimate the product composition as output from the neural network. It is seen from the block diagram that the actual product composition is compared with the reference composition to generate the error. This error is given as the input to a PID controller which is designed to compensate for the error and give the desired reboiler heat duty to regulate the product composition.

Cascade Control Strategy

The block diagram of the proposed cascade control strategy is shown in Figure 7. As compared to single loop control strategy, this control strategy involves two cascaded control loops including composition and temperature control. In this case also, four inputs are given to get six temperatures as output from the system. These four inputs are reflux ratio, feed flow rate FA, and FB and reboiler heat duty. Bottom stage temperature T9 and reboiler heat duty are selected as the manipulated variables to operate both inner and outer loops. Bottom most temperature T9 was selected as manipulated variable because this T9 temperature instantly changes after single loop completes and reboiler heat duty regulated. This change in T9 temperature then helps maintaining product composition. Again, product composition is selected as the controlled variable.

In this cascaded control strategy, the error signal between reference composition ' X_{dref} ' and actual composition ' X_d ' is used to calculate the reference temperature for the bottom plate ' $T9_{ref}$ '. This reference temperature of the T9 plate is then compared with the actual sensed temperature of 9th plate. In this strategy, T9 temperature will track the reference temperature and the product composition will track the reference composition. However, the main condition is that inner loop must be faster as compared to the outer loop. Double loop cascaded control strategy gives improved dynamic response as compared to single loop control strategy. Two controllers PID and PI are used to compensate both inner and outer loops.

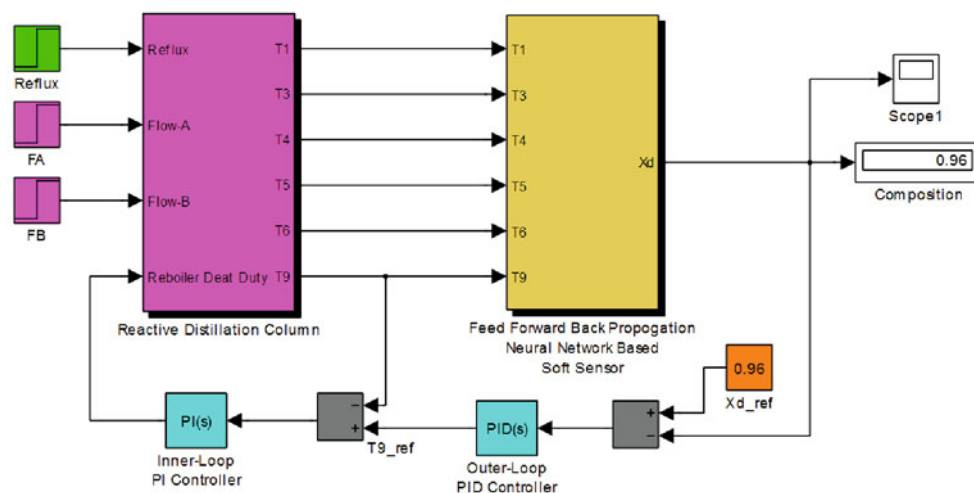


Figure 7. Cascade Control of Reactive Distillation using modified FBPNN

Variation in composition for both single loop and cascaded control strategy is shown in Figure 8. As shown in the figure, the composition variation against time is constant in case of cascaded control strategy. In case of single loop strategy, the variation in composition is increasing continuously and remains constant after 3000 seconds. This response diagram clearly indicates the successful implementation of modified FBPNN as soft sensors estimator for control of such nonlinear reactive distillation column. The range of composition was set between 0.85 to 0.96 and both control strategies were tested by conducting various runs performed in MATLAB.

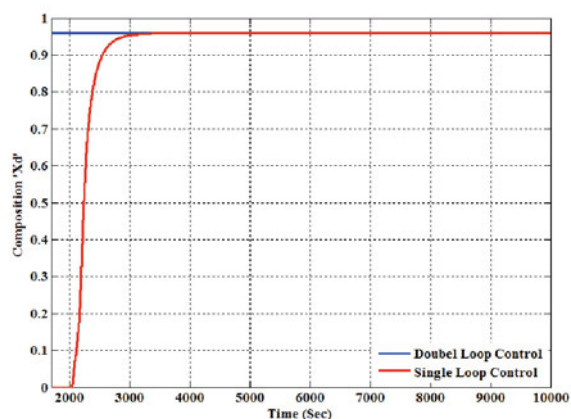


Figure 8. Composition variation against time

Disturbance Rejection and Set Point Tracking

The performance of both single loop and cascaded loop control strategies is tested by applying various disturbances in the system. The $\pm 10\%$ variation in reflux ratio is introduced as input to the system. The estimations obtained from single loop and cascaded loop soft sensor for positive and negative disturbances are shown in Figures 9 and 10 respectively. It is observed that in case of single loop control strategy, the variation in composition is large i.e. the set point changed from 0.96 to 0.9605 and after 600 seconds it comes to steady state (set point). In case of cascaded control, the variation is very small and set point changed from 0.96 to 0.9605 and only after few seconds it reaches steady state.

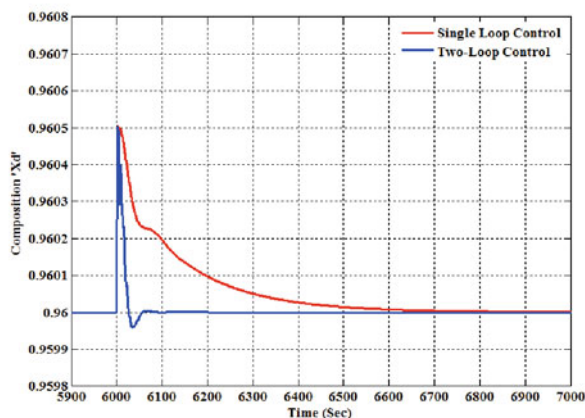


Figure 9. Composition variation after +10% variation in reflux ratio

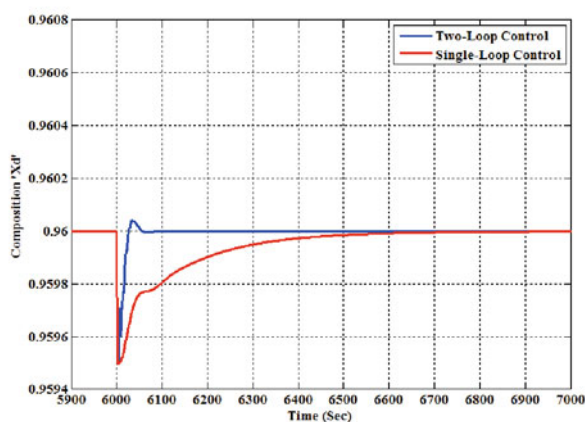


Figure 10. Composition variation after -10% variation in reflux ratio

Similarly, when a step changes of -10% in reflux ratio is given, in case of single loop strategy, again the variation is large, the set point changed from 0.96 to 0.9595 and then after 500 seconds it came back to steady state. In case of cascaded control, the set point changed from 0.96 to 0.9596 and just after a few seconds it reaches steady state.

In the same manner, variation of $\pm 20\%$ in the feed flow rate of component A (FA) is observed. The variation is shown in Figures 11 and 12 respectively. As shown in Figure 11, when a step change of +20% in FA is given, the set point is changed from 0.96 to 0.983, and after

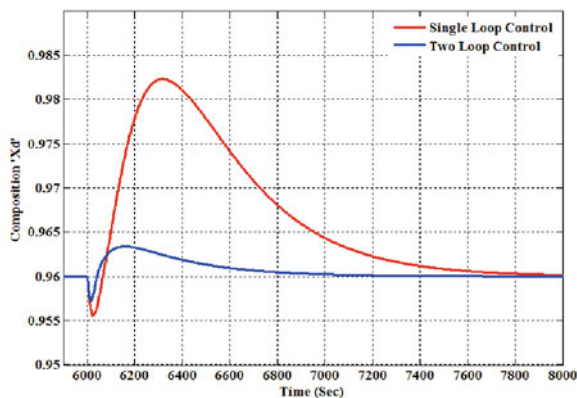


Figure 11. Composition variation after +20% (0.035 to 0.042 l/min) variation in FA

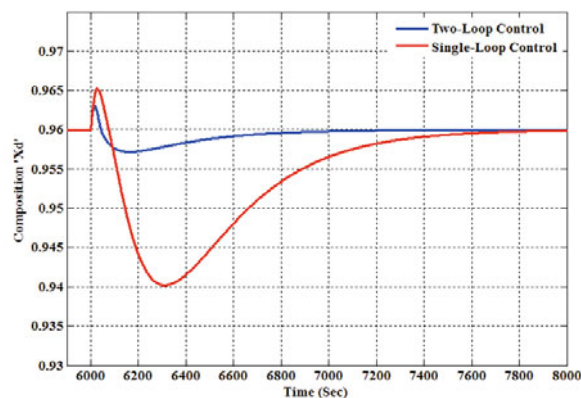


Figure 12. Composition variation after -20% (0.035 to 0.028 l/min) variation in FA

1600 seconds it reached to steady state while in case of cascaded strategy, the set point changed from 0.96 to 0.964, and, then, after 800 seconds only it reached to steady state without much fluctuations. Similarly, when the set point change of -20% is given in the input feed flow rate FA, the set point changed from 0.96 to 0.94 and after 1600 seconds it reached a steady state, while in case of cascaded control, the set point changed from 0.96 to 0.964 and just after a few seconds it reached to steady state.

A similar response is observed when positive variation in set point of feed flow rate FB is given from 0.035 to 0.042 (+20%) and negative variation in set point of FB from 0.035 to 0.028 (-20%) is given and response is shown in Figures 13 and 14 respectively. Again, it is clear from the figure that the dynamic response of cascaded control strategy is excellent as compared to the single loop.

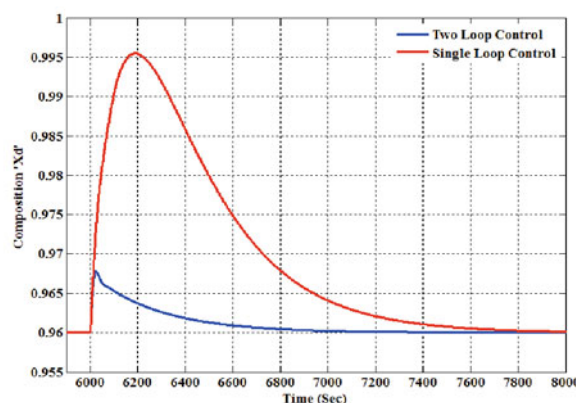


Figure 13. Composition variation after +20% (0.035 to 0.042 l/min) variation in FB

This is also validated when mixed variation in both feed flow rate FA and FB and reflux ratio is given and response for cascaded control obtained is perfect as compared to the single loop. This response curve is shown in Figure 15.

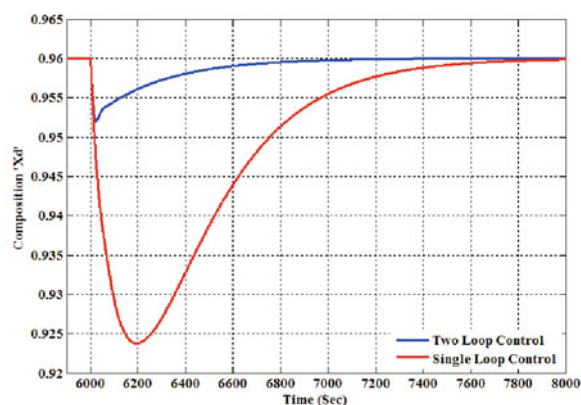


Figure 14. Composition variation after -20% (0.035 to 0.028 l/min) variation in FB

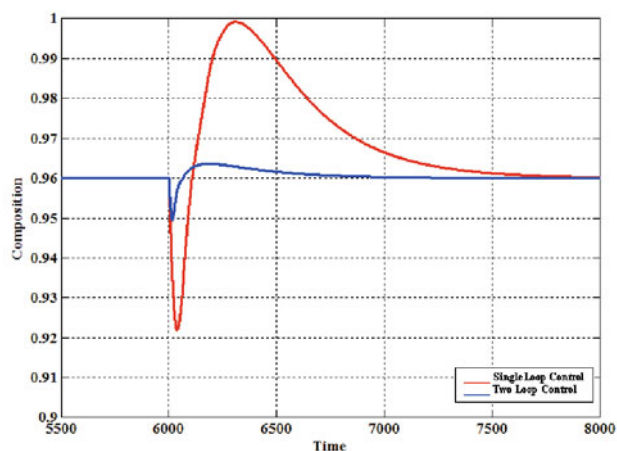


Figure 15. Composition variation against mixed variation in flow (FA+FB)

RESULTS AND DISCUSSION

Simulation Results

A dynamic simulation and control strategy implementation for propyl propionate reactive distillation process is developed in MATLAB (2013b). The simulation runs is carried out in the composition range from 0.85 to 0.96. The composition profile of propyl propionate reactive distillation is shown in Figure 16. It is observed from the graph that product composition obtained is 0.858. As discussed earlier, the product composition obtained experimentally was 0.842. It is showing a good agreement between experimental and simulation results.

Training, Testing and Validation of FBPNN

The training, testing and validation of FBPNN is performed before and after modification of the neural network algorithm. FBPNN without modification of algorithm is first trained using experimental data collected at specified operating condition. Figure 17, old one, is removed from the manuscript.

Training, testing and validation was simultaneously performed for FBPNN algorithm without modification in MATLAB using the same experimental data. For case 1, the number of hidden layer is selected as 10 and training, testing and validation is carried out for one input and one output layer. Figure 17 shows, training, testing and validation for case 1, without modification of

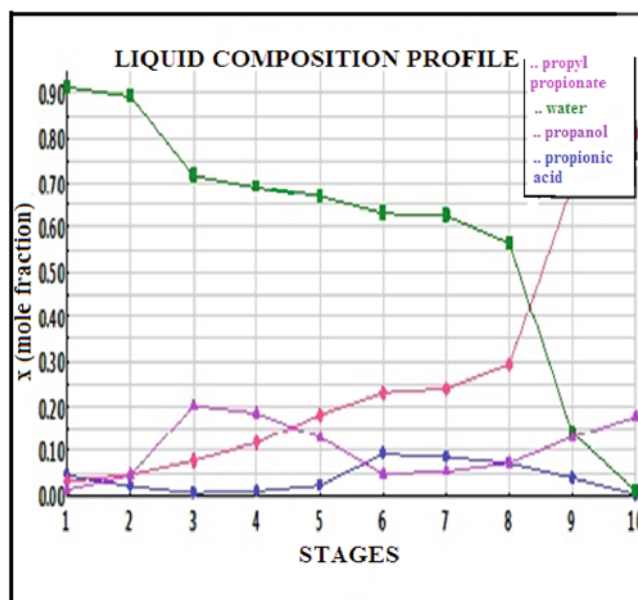


Figure 16. Composition profile of Propyl Propionate

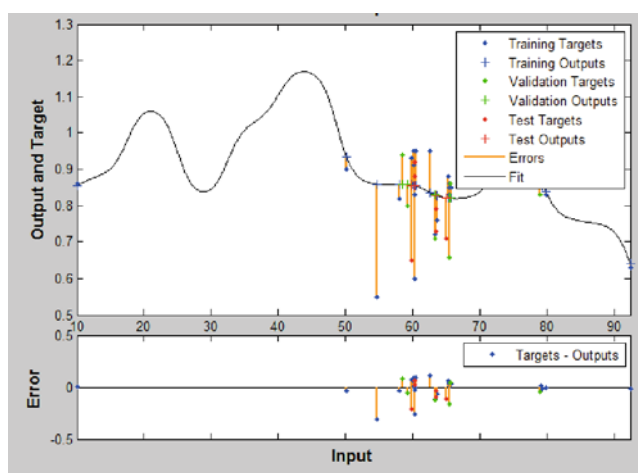


Figure 17. Training, Testing and validation of FBPNN without modification

the algorithm. It is clear from the figure that the error generated for respective output and the target is large.

The product composition as output obtained is 0.86. Similarly, the training, testing and validation is also carried out for the modified FBPNN algorithm. Figure 18 shows the training testing and validation for case 2, in which the number neurons in hidden layer is set

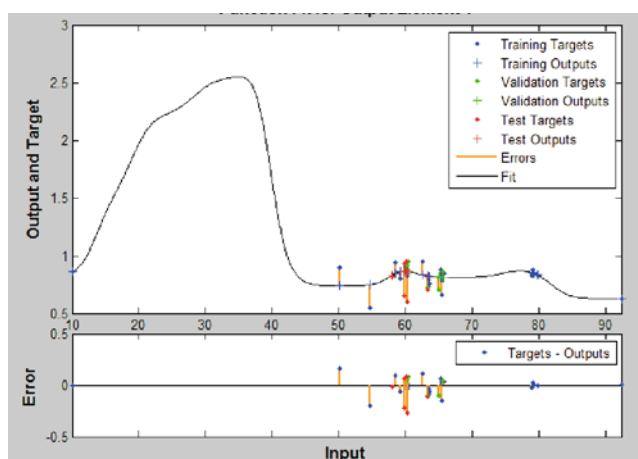


Figure 18. Training, Testing and validation of modified FBPNN

as 12. It is clear from the figure that the error is minimum for algorithm which is modified and optimized for error function.

The performance with mean square error is shown in Figure 19. It is shown in the diagram that training, testing and validation were best performed and the value under circle found as 0.0060659 at epoch 10.

Training, testing and validation of FBPNN algorithm with and without modification is carried out to show that the modification proposed using the steepest descent method for FBPNN algorithm is suitable for error minimization. The mean square error is minimized after modification and helps in improving the performance of the algorithm. This also indicates that the proposed modification in the neural network algorithm is suitable for nonlinear process control application.

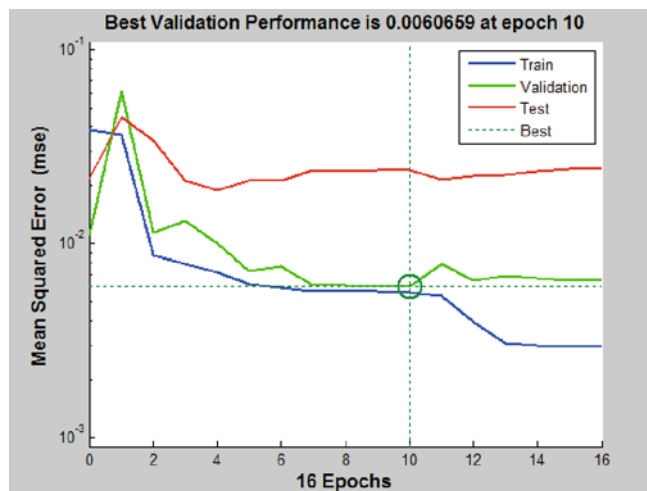


Figure 19. Performance w.r.t to mean square error

Integral Absolute Error (IAE)

Output from a controller is generally located in areas above and below the set point. Integral of absolute error penalize all errors without consideration of direction. The modulus neglects the direction and integrates the error over the process time. IAE is generally used for small deviation process error. In general, the integral absolute error can be given as:

$$IAE = \int_0^t (y - y_{sp}) dt \quad (32)$$

Where, y is the actual output and y_{sp} is the set point. The IAE values are given in Table 2.

CONCLUSION

In this research work, modified FBPNN using the steepest descent method based single loop and cascaded control strategies is proposed for control of propyl propionate reactive distillation column. The proposed modification is used to minimize the mean square error by optimization of weights between input-hidden and hidden-output layer. The proposed single loop control scheme consists of FBPNN estimator and PID controller while the cascaded control scheme consists of FBPNN estimator and two PID controllers for inner and outer loops. The propyl propionate reactive distillation column is modeled and simulated in MATLAB. Experimental data have been collected for temperature and composition. These temperature measurements have been used as a secondary process variable for composition estimation. The limit of the composition estimation was set between 0.86 to 0.96 and several simulation experiments conducted to evaluate the performance of the proposed control scheme. A comparison was made between single loop and cascaded control scheme. It has been observed that the proposed modification of the algorithm is successful in minimization of mean square error and, hence, the performance of the neural network was improved. It has also been observed that the cascaded control scheme gives an improved dynamic response in comparison to single loop. The performance is checked out for various disturbances in input variables and set point tracking. The Mean Square Error (MSE) and Integral Absolute Error (IAE) were also calculated.

NOMENCLATURE

- B – Bottom Flow rate [moles/min]
- C_{H_2O} – Concentration of water [moles]
- C_p – Specific heat of product liquid [J/mole °C]
- C_{PA} – Concentration of propionic acid [moles]
- C_{POH} – Concentration of propanol [moles]
- C_{PP} – Concentration of propyl propionate [moles]
- D – Distillate flow rate [moles/min]
- E_k – Total catalyst volume available in the contacting cell [cm³]
- F_n – Input feed flow rate on nth stage [moles/min]
- h_{n-1} – Enthalpy of liquid at n-1th stage [J]
- H_{n+1} – Enthalpy of vapor at n+1th stage [J]
- h_n – Enthalpy of liquid at nth stage [J]
- H_n – Enthalpy of vapor at nth stage [J]
- h_f – Enthalpy of Feed [J]
- h_R – Enthalpy of liquid accumulated in reactive zone [J]
- h_D – Enthalpy of distillate [J]
- h_B – Enthalpy of bottom product [J]
- H_B – Enthalpy of vapor leaving the reboiler [J]

Table 2. IAE of PID controller subjected to various set point changes

| Manipulating variable | Tuning rule | Step change | Gain | Integral time [mins] | Derivative time [mins] | IAE error |
|-----------------------|---------------|-------------|-------|----------------------|------------------------|-----------|
| Reboiler heat duty | Tyreus Luyben | +10% | 205 | 7 | 0.85 | 0.0050 |
| | | -10% | 185 | 8.2 | 1.27 | 0.0010 |
| Flow rate of feed A | Tyreus Luyben | +10% | 193.3 | 13.20 | 0.01 | 0.0135 |
| | | -10% | 122.3 | 19.8 | 0.52 | 0.0140 |
| Flow rate of feed B | Tyreus Luyben | +10% | 557.1 | 13.2 | 0.16 | 0.0034 |
| | | -10% | 537.2 | 13.2 | 0.45 | 0.0054 |
| Reflux ratio | Tyreus Luyben | +10% | 196 | 9.4 | 0.04 | 0.0012 |
| | | -10% | 185 | 7.2 | 0 | 0.0017 |

ΔH_v – heat due to vaporization [J]
 K_f – forward rate constant [sec^{-1}]
 K_r – Backward rate constant [sec^{-1}]
 K_{eq} – equilibrium rate constant for the reaction [ratio of k_f/k_r]
 L_{n+1} – Liquid flow rate of $n+1^{\text{th}}$ stage [moles/min]
 L_n – Liquid flow rate on n^{th} stage [moles/min]
 M_B – Reboiler holdup [moles]
 M_D – Holdup of distillate [moles]
 M_f – Holdup of feed [moles]
 M_n – Liquid holdup on n^{th} stage [moles]
 Q_C – Condenser Heat duty [kW]
 Q_B – Reboiler Heat duty [kW]
 RR – Reflux ratio [constant]
 R – Universal gas constant [(atm · cm³)/(gmole K)]
 R_{rate} – Reflux rate [mole/min]
 $R_{n,i}$ – Net reaction rate of component i on n^{th} stage [(mole)(litre⁻¹)(sec⁻¹)]
 T_n – Temperature for n^{th} stage [°C]
 T_{n+1} – Temperature for $n+1^{\text{th}}$ stage [°C]
 T_{n-1} – Temperature for $n-1^{\text{th}}$ stage [°C]
 T_{feed} – Temperature of feed stream [°C]
 T_f – Temperature of feed plate [°C]
 T_R – Average Temperature of reaction zone [°C]
 T – Reaction Temperature [°C]
 V_n – Vapor flow rate on n^{th} stage [moles/min]
 V_{n-1} – Vapor flow rate on $n-1^{\text{th}}$ stage [moles/min]
 V_B – Flow rate of vapor leaving the reboiler [moles/min]
 V_R – Volume of Reactive Zone [m³]
 $v_{i,m}$ – Stoichmetric coefficient of component i [constant]
 V_M – Volume through which mass transfer occur [m³]
 W – Mass of dry catalyst used [g]
 $x_{D,i}$ – Composition of distillate
 $x_{n,i}$ – Liquid composition of component i on n^{th} tray
 $x_{B,i}$ – Liquid composition of bottom product
 $x_{n+1,i}$ – Liquid composition of component i on $n+1^{\text{th}}$ tray
 $y_{n-1,i}$ – Vapor composition of component i on $n-1^{\text{th}}$ tray
 $y_{n,i}$ – Vapor composition of component i on n^{th} tray
 $y_{B,i}$ – Composition of vapor leaving the reboiler
 $z_{n,i}$ – Feed composition of component i on n^{th} tray
 λ – Latent heat of reaction [J/mole]

ACKNOWLEDGEMENT

The author thankfully acknowledges the financial assistance provided by the All India Council for Technical Education (AICTE), New Delhi (INDIA), under the Research Promotion Scheme (RPS).

LITERATURE CITED

- Sorensen, E., Macchieto, S., Stuart, G. & Skogestad, S. (1996). Optimal Control and Online Operation of Reactive Batch Distillation, *Comput. & Chem. Eng.* 20, 1491–1498. DOI: 10.1016/0098-1354(95)00234.
- Al-Arfaj, M. & Luyben, W.L. (2000). Comparison of Alternative Control Structures for an Ideal Two-Product Reactive Distillation Column. *Ind. Eng. Chem. Res.* 39, 3298–3307. DOI: 10.1021/ie 990886j.
- Kano, M., Miyazaki, K., Hasebe, S. & Hashimoto, I. (2000). Inferential Control System of Distillation Compositions using Dynamic Partial Least Squares Regression. *J. Proc. Cont.* 10, 157–166. DOI: 10.1016/50959-1524(99)00027-x.
- Balasubramhanya, L.S. & Doyle III, F.J. (2000). Nonlinear Model Based Control of a Batch Reactive Distillation Column. *J. Proc. Cont.* 10, 209–218. DOI: 10.1016/50959-1524 (99) 00024-4.
- Tian, Yu-Chu, Zhao, F., Bisowarno, B.H. & Tade, M.O. (2003). Pattern-Based Predictive Control for ETBE Reactive Distillation. *J. Proc. Cont.* 13, 57–67. DOI: 10.106/50959-1524(02)00011-2.
- Hung, Shih-Bo & Lee, M.J. (2005). Control of Different Reactive Distillation Configuration. *Wiley Inter. Sci.* 52, 1423–1440. DOI: 10.1002/aic.10743.
- Lai, K., Hung, S.B., Hung, W.J., Yu, C.C., Lee, M.J. & Huang, H.P. (2007). Design and control of reactive distillation for ethyl and isopropyl acetates production with azeotropic feeds. *Chem. Engineer. Sci.* 62, 878–898. DOI: 10.1016/j.ces.2006.10.019.
- Chien, I-Lung., Chen, K. & Kuo, C.L. (2008). Overall control strategy of a coupled reactor/columns process for the production of ethyl acrylate. *J. Proc. Cont.* 18, 215–231. DOI: 10.1016/j.jprocont.2007.02.006.
- Wang, San-Jang., Yu, C.C. & Huang H.P. (2010). Steady-state design of thermally coupled reactive distillation process for the synthesis of Diphenyl carbonate, *Computers and Chemical Engineering*, 34, 361–373. DOI:10.1016/j.compchemeng.2013.02.001.
- Wei, Hon-Yu., Rokhmah, A., Handogo, R. & Chien, I.H. (2011). Design and control of reactive- distillation process for the production of diethyl carbonate via two consecutive trans-esterification reactions, *Journal of Process Control*, 21, 1193–1207. DOI: 10.1016/2011.06.006.
- Wu, Yi-Chang., Lee, H.Y., Tsai, C.Y., Huang, H.P. & Chien, I.H. (2013). Design and control of a reactive-distillation process for esterification of an alcohol mixture containing ethanol and n-butanol. *Comput. Chem. Engine.* 57, 63–67. DOI: 10.1016/2013.01.002.
- Mahindrakar, V. & Hahn, J. (2014). Dynamics and control of benzene hydrogenation via reactive distillation. *J. Proc. Cont.* 24, 113–124. DOI: 10.1016/2014.01.005.
- Brasio, A.S.R., Romanenko, A., Leal, J., Santos, L.O. & Fernandes, N.C.P. (2013). Nonlinear model predictive control of biodiesel production via transesterification of used vegetable oils. *J. Proc. Cont.* 23, 1471–1479. DOI: 10.1016/2013.09.023.
- Li, W., Hung, K., Zhang, L., Chen, H. & Wang, S.J. (2012). Dynamics and control of totally refluxed reactive distillation columns. *J. Proc. Cont.* 22, 1182–1197. DOI: 10.1016/2012.05.007.
- Sumana, C. & Venkateswarlu, C. (2007). Development of a software sensor for compositions in continuous reactive distillation, *J. Sci. & Indust. Res.* 66, 898–904.
- Kathel, P. & Jana, A.K. (2010). Dynamic simulation and nonlinear control of a rigorous batch reactive distillation. *ISA Transact.* 49, 130–137. DOI: 10.1016/2009.09.007.
- Prakash, K.J.J., Patle, D.S. & Jana, A.K. (2011). Neuro-estimation based GMC control of a batch reactive distillation, *ISA Transact.* 50, 357–363. DOI: 10.1016/2011.01.010.
- Raghavan, S.R.V., Radhakrishnan, T.K. & Srinivasan, K. (2011). Soft sensor based composition estimation and controller design for an ideal reactive distillation column. *ISA Transact.* 50, 61–70. DOI: 10.1016/2010.09.001.
- Rani, A., Singh, V. & Gupta, J.R.P. (2011). Soft Sensor based Adaptive Linear Network for Distillation Process. *Inter. J. Comput. Applicat.* 36, 39–45. DOI: 10.5120/4458-6244.
- Canete, J.F. de, Orozco, P. del S., Gonzalez, S. & Moral, I.G. (2012). Dual composition control and soft estimation for a pilot distillation column using a neuro-genetic design. *Comput. Chem. Engine.* 40, 157–170. DOI: 10.1016/j.compchemeng.2012.01.003.
- Sharma, N. & Singh, K. (2012). Model predictive control and neural network predictive control of TAME reactive distillation column. *Chem. Engine. Proces.* 1–13. DOI: 10.1016/j.ccep.2012.05.003.

22. Rani, A., Singh, V. & Gupta J.R.P. (2013). Development of soft sensor for neural network based control of distillation column. *ISA Transact.* 52, 438–449. DOI: 10.1016/2012.12.009.
23. Duarte, C.F.M. (2006). *Production of TAME and n-Propyl Propionate by Reactive Distillation*, Doctoral Dissertation, Faculty of Engineering of the University of Porto, Porto, Portugal.
24. Buchaly, C., Kreis, P. & Gorak, A. (2007). Hybrid Separation Process- Combination of Reactive Distillation with Membrane Separation, *Proceedings of European congress of Chemical Engineering (ECCE-6)*, 4–5.
25. Sivanandam, S.N. & Deepa, S.N. (2011). *Principles of Soft Computing*, second edition, Wiley India.
26. Astrom, K.J. & Hagglund, T. (1995). *PID Controllers: Theory, Design and Tuning*, second edition, ISA publication.